

Optimal Front-End Design for MIMO Receivers

Carlo P. Domizioli, Brian L. Hughes, Kevin G. Gard and Gianluca Lazzi

Department of Electrical and Computer Engineering

North Carolina State University

Raleigh, NC 27695-7914

{cpdomizi,blhughes,kevin_gard,lazzi}@ncsu.edu

Abstract—The effect of antenna mutual coupling on fading correlation in compact MIMO arrays has received considerable attention. By contrast, relatively little attention has been paid to the noise. In this paper we present a circuit model for a noisy MIMO receiver front-end that includes arbitrary coupling and noise correlation. The noise figure for two-port networks is extended to multiport networks, from which theorems for optimal front-end design are derived. Numerical results are presented which provide insight into receiver noise behavior in the presence of coupled antennas.

I. INTRODUCTION

The capacity of a fading wireless channel may be substantially increased by employing multiple antennas at both the transmitter and receiver, resulting in a multiple-input, multiple-output (MIMO) channel. As with any communication system, developing an accurate yet mathematically tractable channel model is essential to predicting the performance of actual systems. Since the seminal papers of Telatar [1] and Foschini and Gans [2], which assumed independent fading between each transmit and receive antenna, there has been an enormous amount of research devoted to this subject.

Initial studies in this area examined the impact of fading correlation by developing ray-tracing and analytical correlation models and evaluating their effect on capacity through Monte Carlo simulations, asymptotic analysis, and bounding techniques (examples of each of these may be found in several special issues on the subject [3]- [5]). The results generally indicate a loss in performance with correlation, however, in sufficiently rich scattering environments the antenna separations may be made as small as half a wavelength without significant performance degradation (cf., [6]). At such small spacings the antennas may become coupled, so the ensuing studies (cf., [7] and the references within) analyzed the impact of mutual coupling on fading correlation. This led to the consideration of matching networks to maximize the transfer of power from the coupled array to the rest of the receiver [8].

While these studies introduced increasing detailed models of the fading correlation, little attention was paid to the noise. In fact, most of the papers cited above assume a spatially white noise model, only mentioning noise correlation in reference to interference (cf., [9]). However, for closely-spaced antennas even noise generated in the receiver may become correlated.

For example, noise in a front-end amplifier may disperse across neighboring receiver chains through coupled antennas.

A non-trivial noise model for a MIMO receiver was considered in [10], where the authors introduced a standard amplifier model into their previous model for mutual coupling [8]. They demonstrated that matching networks optimized for noise figure outperformed those designed for maximum power transfer. More recently, Gans [11], [12] evaluated the impact of antenna thermal noise and (spatially white) amplifier noise individually. It was shown that matching networks offer no improvement in capacity when antenna noise is dominant, while they are essential when amplifier noise is dominant.

In this paper we establish low-noise design principles for coupled MIMO receivers. After obtaining an expression for capacity with spatially correlated noise, we introduce a front-end circuit model that includes arbitrary coupling and noise correlation between its branches. By extending the well-known concept of noise figure for two-port networks to multiport networks, we are able to derive theorems for optimal front-end design. Finally, we present some numerical examples that illustrate the theory. In one particularly surprising example we present two front-ends with the same noise figure that produce remarkably different capacities in the presence of coupled antennas. A brief review of some relevant concepts from two-port noise modeling is provided in the Appendix.

II. MIMO CAPACITY WITH CORRELATED NOISE

A frequency-flat MIMO system with N transmit and M receive antennas may be modeled as

$$\mathbf{r} = \mathbf{H}\mathbf{x} + \mathbf{n}, \quad (1)$$

where $\mathbf{x} \in \mathbb{C}^N$ is the transmitted signal; $\mathbf{r}, \mathbf{n} \in \mathbb{C}^M$ are the received signal and noise, respectively; and $\mathbf{H} \in \mathbb{C}^{M \times N}$ is the channel matrix. The transmitter is constrained in power by $\text{tr}(\mathbb{E}[\mathbf{x}\mathbf{x}^\dagger]) \leq P$, where $\text{tr}(\cdot)$ and $\mathbb{E}[\cdot]$ are the trace and expectation, and \dagger denotes the conjugate-transpose. We assume Rayleigh fading and a Kronecker correlation model [6] with no transmit correlation, so the columns of \mathbf{H} are independent and identically distributed (i.i.d.) zero-mean, circularly-symmetric, complex Gaussian random vectors, denoted by $\mathbf{h}_i \sim \mathcal{CN}(\mathbf{0}, \mathbf{\Sigma}_h)$, where $\mathbf{\Sigma}_h = \mathbb{E}[\mathbf{h}_i\mathbf{h}_i^\dagger]$ is the correlation matrix. We assume \mathbf{H} is known at the receiver but not the transmitter. The noise is also Gaussian with spatial correlation, so $\mathbf{n} \sim \mathcal{CN}(\mathbf{0}, \mathbf{\Sigma}_n)$. Most prior work on MIMO assumes spatially white noise, so $\mathbf{\Sigma}_n \propto \mathbf{I}$ where \mathbf{I} is the identity matrix.

¹This material is based upon work supported by the National Science Foundation under grants CCF-0312686 and CCF-0515164.

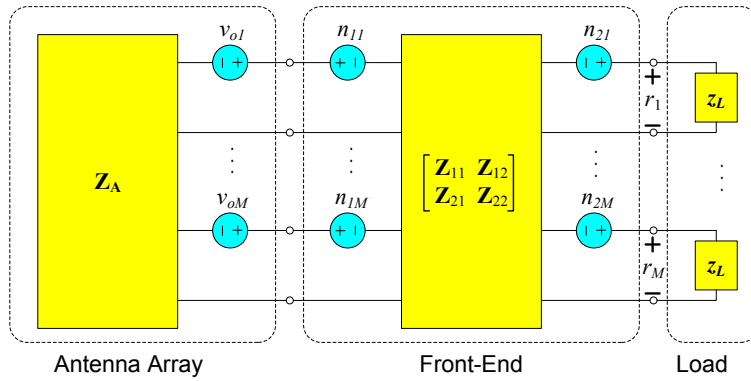


Fig. 1. Receiver model. The antenna array and front-end are modeled with Thevenin equivalent networks.

The ergodic capacity of this system may be obtained from the familiar formula for spatially white noise [6] by applying a noise-whitening filter $\Sigma_{\mathbf{n}}^{-1/2}$ to \mathbf{r} , which will not affect the capacity. The ergodic capacity is then

$$C = \mathbb{E} [\log \det (\mathbf{I} + \mathbf{H}_w^\dagger \Sigma \mathbf{H}_w)] , \quad (2)$$

where $\mathbf{H}_w \in \mathbb{C}^{M \times N}$ has i.i.d. $\mathcal{CN}(0, 1)$ entries,

$$\Sigma \triangleq \frac{P}{N} \Sigma_{\mathbf{h}}^{1/2} \Sigma_{\mathbf{n}}^{-1} \Sigma_{\mathbf{h}}^{1/2} , \quad (3)$$

and $\mathbf{A}^{1/2}$ denotes the positive definite square root of a positive definite matrix \mathbf{A} [13, pg. 406]. We will refer to Σ as the *SNR matrix* as it is analogous to the signal-to-noise ratio (SNR) of a single-input, single-output (SISO) system.

A closed-form expression for (2) was derived in [14]. In particular, if $M = N$ and Σ has distinct eigenvalues $\lambda_1 > \lambda_2 > \dots > \lambda_N > 0$, this expression reduces to

$$C = \frac{\sum_{k=1}^N \det \mathbf{A}_k}{\prod_{\substack{i=1 \\ j>i}}^N \lambda_i^i (1 - \lambda_i/\lambda_j)} \quad (4)$$

where $\mathbf{A}_k \in \mathbb{R}^{N \times N}$ is defined by

$$[\mathbf{A}_k]_{ij} = \begin{cases} \frac{1}{(j-1)!} \int_0^\infty u^{j-1} e^{-u/\lambda_i} \log(1+u) du, & j = k \\ \lambda_i^j, & j \neq k \end{cases}$$

The only case of non-distinct eigenvalues we shall consider is $\Sigma = \frac{\rho}{N} \mathbf{I}$, for which Telatar's expression [1] applies:

$$C = \sum_{k=0}^{N-1} \int_0^\infty L_k^2(u) e^{-u} \log \left(1 + \frac{\rho}{N} u \right) du , \quad (5)$$

where $L_k(u)$ is the Laguerre polynomial of order k .

III. RECEIVER MODEL

The signal received by the antennas is usually amplified and down-converted before A/D conversion and digital signal processing. The analog circuits that accomplish this goal are collectively referred to as the *front-end*. We shall take (1) as the voltage input to the A/D converters and \mathbf{n} as the collective effect of thermal noise from the antennas and (thermal and non-thermal) noise generated in the front-end. The antennas

and front-end are assumed to be frequency-flat over the system bandwidth and are modeled by Thevenin equivalent networks, as shown in Fig. 1, where the load is the A/D converter input impedance. Below we discuss these networks in more detail.

A. Antenna Array

Let $\mathbf{v}, \mathbf{i} \in \mathbb{C}^M$ denote the voltage across and current flowing into the antenna array terminals, respectively. The circuit equation for the array is (cf., [15])

$$\mathbf{v} = \mathbf{Z}_A \mathbf{i} + \mathbf{v}_o , \quad (6)$$

where $\mathbf{Z}_A = \mathbf{R}_A + j\mathbf{X}_A$ is the antenna impedance matrix and \mathbf{v}_o is the open-circuit voltage, as shown in Fig. 1. For a uniform linear array (ULA), \mathbf{Z}_A is a function¹ of the inter-element spacing d . Mutual coupling between the antennas is reflected by the off-diagonal elements of \mathbf{Z}_A . The open-circuit voltage is related to the incident electric field by the array radiation pattern and, since the front-end is linear, takes the same form as (1),

$$\mathbf{v}_o = \mathbf{H}_o \mathbf{x} + \mathbf{n}_o , \quad (7)$$

where the columns of \mathbf{H}_o are i.i.d. and Gaussian.

Nyquist's formula for thermal noise applies to an antenna when it is enclosed by a black-body radiator [17, pg. 111]. This formula was extended to antenna arrays by Twiss [18], who showed that the noise voltage can be modeled as $\mathbf{n}_o \sim \mathcal{CN}(\mathbf{0}, 4kT_0 B \mathbf{R}_A)$, where $k = 1.38 \times 10^{-23}$ J/K is Boltzmann's constant, $T_0 = 290$ K is the standard temperature, and B is the bandwidth in Hz. Note that with the array imbedded in a linear medium, the reciprocity theorem (cf., [16, pg. 144]) applies so that \mathbf{Z}_A is symmetric.

B. Front-End

Most prior studies of noise in MIMO receivers have been restricted to uncoupled amplifiers [10], [12]. Here we take a more general viewpoint and assume the front-end may have arbitrary coupling and noise correlation between its ports. Let $\mathbf{v}_1, \mathbf{v}_2 \in \mathbb{C}^M$ and $\mathbf{i}_1, \mathbf{i}_2 \in \mathbb{C}^M$ denote the voltages and currents

¹Approximate formulas are available for infinitesimally-thin wire dipoles; other antennas may be evaluated using numerical techniques [16, ch. 8].

at the input and output terminals of the front-end in Fig. 1, respectively. These circuit quantities are related by

$$\begin{bmatrix} \mathbf{v}_1 \\ \mathbf{v}_2 \end{bmatrix} = \begin{bmatrix} \mathbf{Z}_{11} & \mathbf{Z}_{12} \\ \mathbf{Z}_{21} & \mathbf{Z}_{22} \end{bmatrix} \begin{bmatrix} \mathbf{i}_1 \\ \mathbf{i}_2 \end{bmatrix} + \begin{bmatrix} \mathbf{n}_1 \\ \mathbf{n}_2 \end{bmatrix}, \quad (8)$$

where $\mathbf{Z}_{ij} \in \mathbb{C}^{M \times M}$, and the noise voltages $\mathbf{n}_1, \mathbf{n}_2$ are zero-mean Gaussian with correlation matrices $\boldsymbol{\Sigma}_{ij} \triangleq \mathbb{E}[\mathbf{n}_i \mathbf{n}_j^\dagger]$.

Solving the circuit in Fig. 1 for the output voltage, we obtain

$$\mathbf{r} = \left[z_L \left(\mathbf{Z}_{22} + z_L \mathbf{I} - \mathbf{G} \mathbf{Z}_{12}^\dagger \right)^{-1} \mathbf{G} \right] (\mathbf{v}_o - \mathbf{n}_1 + \mathbf{G}^{-1} \mathbf{n}_2),$$

where $\mathbf{G} = \mathbf{Z}_{21} (\mathbf{Z}_A + \mathbf{Z}_{11})^{-1}$ and we have assumed the impedance matrices are nonsingular. The term inside the square brackets multiplies both the signal and noise components of \mathbf{r} , which will result in a similarity transformation on the SNR matrix $\boldsymbol{\Sigma}$. Since (2) depends only on the eigenvalues of $\boldsymbol{\Sigma}$, this will not alter the capacity and we may take

$$\mathbf{r} = \mathbf{H}_o \mathbf{x} + \mathbf{n}_o + \mathbf{z}, \quad (9)$$

where $\mathbf{z} = \mathbf{G}^{-1} \mathbf{n}_2 - \mathbf{n}_1$ is noise from the front-end. Comparing (1) and (9) we see that the model of Fig. 1 maps to the standard model (1) with $\mathbf{H} = \mathbf{H}_o$ and $\mathbf{n} = \mathbf{n}_o + \mathbf{z}$. Intuitively, (9) refers all voltages to the open-circuited antenna terminals.

IV. THE NOISE FACTOR MATRIX

The noise factor of a two-port network is the ratio of the output noise power to the noise power contributed by a thermal source alone (cf., Appendix). This concept may be extended to multiport networks by defining the *noise factor matrix*

$$\begin{aligned} \mathbf{F} &\triangleq (\boldsymbol{\Sigma}_{\mathbf{n}|z=0})^{-1/2} \boldsymbol{\Sigma}_{\mathbf{n}} (\boldsymbol{\Sigma}_{\mathbf{n}|z=0})^{-1/2} \\ &= \mathbf{I} + \frac{1}{4kT_0 B} \mathbf{R}_A^{-1/2} \mathbb{E}[\mathbf{z} \mathbf{z}^\dagger] \mathbf{R}_A^{-1/2}. \end{aligned} \quad (10)$$

The two-port noise factor is useful since it equals the SNR drop across the network. Thus, from a system design perspective, the noise factor provides a sufficient description of a device and we may ignore its internal details. As we shall see, \mathbf{F} enjoys similar properties. Indeed, (3) may be expressed as

$$\boldsymbol{\Sigma} = \frac{P}{4kT_0 B N} \boldsymbol{\Sigma}_{\mathbf{h}}^{1/2} \mathbf{R}_A^{-1/2} \mathbf{F}^{-1} \mathbf{R}_A^{-1/2} \boldsymbol{\Sigma}_{\mathbf{h}}^{1/2}. \quad (11)$$

The noise factor of a two-port should be made as small as possible so that the output SNR (and hence capacity) is maximized, as discussed in the Appendix. Since $\boldsymbol{\Sigma}_{\mathbf{h}}, \mathbf{R}_A$ and \mathbf{F} are positive definite, we may extend this concept to multiport networks using the positive semidefinite partial ordering [13, pg. 469]. For $\mathbf{A}, \mathbf{B} \in \mathbb{C}^{M \times M}$ and Hermitian, we use the notation $\mathbf{A} \geq \mathbf{B}$ and $\mathbf{A} > \mathbf{B}$ to indicate that $\mathbf{A} - \mathbf{B}$ is positive semidefinite and positive definite, respectively.

Theorem 1: Suppose two otherwise identical MIMO systems have front-ends with noise factor matrices $\mathbf{F}_1 \leq \mathbf{F}_2$. Then the corresponding capacities satisfy $C_1 \geq C_2$, with equality if and only if $\mathbf{F}_1 = \mathbf{F}_2$.

Proof: We first claim that if $\mathbf{A} \geq \mathbf{B} > \mathbf{0}$ are Hermitian matrices then $\log \det \mathbf{A} \geq \log \det \mathbf{B}$, with equality if and only

if $\mathbf{A} = \mathbf{B}$. To prove this, observe that $\mathbf{C} \triangleq \mathbf{B}^{-1/2} \mathbf{A} \mathbf{B}^{-1/2} \geq \mathbf{I}$ implies that the eigenvalues of \mathbf{C} satisfy $\lambda_i \geq 1$. Thus

$$\log \det \mathbf{C} = \log \det \mathbf{A} - \log \det \mathbf{B} = \sum_i \log \lambda_i \geq 0, \quad (12)$$

with equality if and only if $\lambda_i = 1$ for each i . Since \mathbf{I} is the only Hermitian matrix that satisfies these conditions, equality holds if and only if $\mathbf{C} = \mathbf{I}$, or equivalently $\mathbf{A} = \mathbf{B}$.

Now let $\mathbf{F}_1 \leq \mathbf{F}_2$ be any noise factor matrices and let $\boldsymbol{\Sigma}_1$ and $\boldsymbol{\Sigma}_2$ denote the corresponding SNR matrices in (11). Since $\mathbf{F}_1 \leq \mathbf{F}_2$ implies $\boldsymbol{\Sigma}_1 \geq \boldsymbol{\Sigma}_2$, for all \mathbf{H}_w we therefore have

$$\mathbf{I} + \mathbf{H}_w^\dagger \boldsymbol{\Sigma}_1 \mathbf{H}_w \geq \mathbf{I} + \mathbf{H}_w^\dagger \boldsymbol{\Sigma}_2 \mathbf{H}_w > \mathbf{0}. \quad (13)$$

Applying the claim above, we conclude

$$\log \det(\mathbf{I} + \mathbf{H}_w^\dagger \boldsymbol{\Sigma}_1 \mathbf{H}_w) \geq \log \det(\mathbf{I} + \mathbf{H}_w^\dagger \boldsymbol{\Sigma}_2 \mathbf{H}_w) \quad (14)$$

with equality if and only if $\mathbf{H}_w^\dagger (\boldsymbol{\Sigma}_1 - \boldsymbol{\Sigma}_2) \mathbf{H}_w = \mathbf{0}$.

From (2), we conclude $C_1 \geq C_2$. Note $C_1 = C_2$ only if equality holds in (14) with probability one in the distribution of \mathbf{H}_w . This in turn holds only if $\mathbf{H}_w^\dagger (\boldsymbol{\Sigma}_1 - \boldsymbol{\Sigma}_2) \mathbf{H}_w = \mathbf{0}$ with probability one, which implies $\mathbb{E}[\mathbf{H}_w^\dagger (\boldsymbol{\Sigma}_1 - \boldsymbol{\Sigma}_2) \mathbf{H}_w] = \text{tr}(\boldsymbol{\Sigma}_1 - \boldsymbol{\Sigma}_2) \mathbf{I} = \mathbf{0}$. Since $\boldsymbol{\Sigma}_1 \geq \boldsymbol{\Sigma}_2$, the eigenvalues μ_i of $\boldsymbol{\Sigma}_1 - \boldsymbol{\Sigma}_2$ are nonnegative and $\sum_i \mu_i = \text{tr}(\boldsymbol{\Sigma}_1 - \boldsymbol{\Sigma}_2) = 0$, so $\mu_i = 0$ for all i and hence $\boldsymbol{\Sigma}_1 = \boldsymbol{\Sigma}_2$. We conclude $C_1 = C_2$ if and only if $\boldsymbol{\Sigma}_1 = \boldsymbol{\Sigma}_2$, or equivalently $\mathbf{F}_1 = \mathbf{F}_2$. ■

V. OPTIMAL MATCHING FOR FRONT-END AMPLIFIERS

Theorem 1 provides a design goal for MIMO front-ends. In this section we apply this to a front-end consisting of a $2M$ -port matching network and a bank of M uncoupled, identical amplifiers, as shown in Fig. 2. Ideally, the matching network is lossless so that it does not dissipate power or generate noise. Such a network satisfies [15, pg. 13] $\mathbf{Z}_{M11} = -\mathbf{Z}_{M11}^\dagger$, $\mathbf{Z}_{M22} = -\mathbf{Z}_{M22}^\dagger$, and $\mathbf{Z}_{M21} = -\mathbf{Z}_{M12}^\dagger$. The amplifiers are represented by Rothe-Dahlke equivalent networks (cf., Appendix) with $\mathbf{v}_a \sim \mathcal{CN}(\mathbf{0}, 4kT_0 B r_a \mathbf{I})$ and $\mathbf{i}_a \sim \mathcal{CN}(\mathbf{0}, 4kT_0 B g_a \mathbf{I})$ mutually independent. Front-ends of this form were considered in [10] and [12], however, in the former antenna thermal noise was neglected and in the latter additional constraints were imposed upon the amplifiers.

After some tedious but essentially straightforward circuit analysis, the front-end noise may be found as

$$\mathbf{z} = \mathbf{M}^{-1} [\mathbf{v}_a + (\mathbf{Z}'_A + z_{\text{cor}} \mathbf{I}) \mathbf{i}_a], \quad (15)$$

$$\mathbf{M} = \mathbf{Z}_{M21} (\mathbf{Z}_A + \mathbf{Z}_{M11})^{-1} \quad (16)$$

$$\mathbf{Z}'_A = -\mathbf{M} \mathbf{Z}_{M12} + \mathbf{Z}_{M22}. \quad (17)$$

Using this in (10), we obtain the noise factor matrix as

$$\begin{aligned} \mathbf{F} &= \mathbf{I} + \mathbf{R}_A^{-1/2} \mathbf{M}^{-1} \left[r_a \mathbf{I} + \right. \\ &\quad \left. g_a (\mathbf{Z}'_A + z_{\text{cor}} \mathbf{I}) (\mathbf{Z}'_A + z_{\text{cor}} \mathbf{I})^\dagger \right] \mathbf{M}^{-\dagger} \mathbf{R}_A^{-1/2} \end{aligned} \quad (18)$$

which reduces to the classical noise factor (25) for $M = 1$. The noise factor of a two-port achieves its minimum F_{\min} (27) when the source impedance is $z_{\text{opt}} = r_{\text{opt}} + jx_{\text{opt}}$ (28). The following theorem extends this result for $M > 1$.

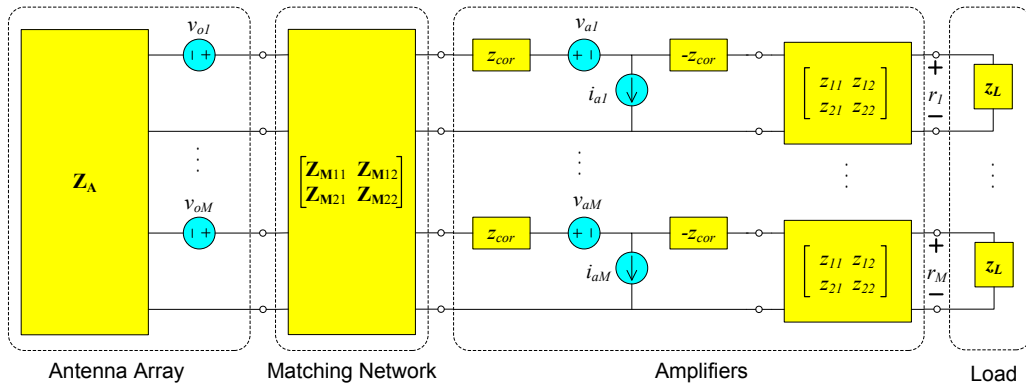


Fig. 2. A simple front-end consisting of a matching network and M uncoupled amplifiers.

Theorem 2: For the noise factor matrix in (18) we have $\mathbf{F} \geq F_{\min} \mathbf{I}$, with equality if and only if $\mathbf{Z}'_{\mathbf{A}} = z_{\text{opt}} \mathbf{I}$. One particular network which achieves the lower bound is

$$\begin{bmatrix} \mathbf{Z}_{\mathbf{M}11} & \mathbf{Z}_{\mathbf{M}12} \\ \mathbf{Z}_{\mathbf{M}21} & \mathbf{Z}_{\mathbf{M}22} \end{bmatrix} = j \begin{bmatrix} -\mathbf{X}_{\mathbf{A}} & (r_{\text{opt}} \mathbf{R}_{\mathbf{A}})^{1/2} \\ (r_{\text{opt}} \mathbf{R}_{\mathbf{A}})^{1/2} & x_{\text{opt}} \mathbf{I} \end{bmatrix}.$$

Proof: Factor the term in the square brackets of (18) as

$$\begin{aligned} r_a \mathbf{I} + g_a (\mathbf{Z}'_{\mathbf{A}} + z_{\text{cor}} \mathbf{I}) (\mathbf{Z}'_{\mathbf{A}} + z_{\text{cor}} \mathbf{I})^\dagger &= \\ g_a (z_{\text{opt}} \mathbf{I} - \mathbf{Z}'_{\mathbf{A}}) (z_{\text{opt}} \mathbf{I} - \mathbf{Z}'_{\mathbf{A}})^\dagger + \frac{F_{\min} - 1}{2} (\mathbf{Z}'_{\mathbf{A}} + \mathbf{Z}'_{\mathbf{A}})^\dagger & \\ \geq \frac{F_{\min} - 1}{2} (\mathbf{Z}'_{\mathbf{A}} + \mathbf{Z}'_{\mathbf{A}})^\dagger &= (F_{\min} - 1) \mathbf{M} \mathbf{R}_{\mathbf{A}} \mathbf{M}^\dagger, \end{aligned}$$

with equality if and only if $\mathbf{Z}'_{\mathbf{A}} = z_{\text{opt}} \mathbf{I}$. Applying this to (18) yields the desired result. The above matching network achieves this minimum and is lossless since $\mathbf{Z}_{\mathbf{A}}$ is symmetric. ■

Matching networks of the above form have appeared elsewhere in the literature (cf., [10] and [12]) without a proof of optimality. From the two theorems established in this paper, we readily see that for any matching network with $\mathbf{Z}'_{\mathbf{A}} \neq z_{\text{opt}} \mathbf{I}$ capacity is strictly less than that achieved by optimal matching.

VI. NUMERICAL RESULTS

With the analytical portion of our paper complete, we present some numerical results to illustrate our theory. We first describe the antenna array and propagation model, then evaluate capacity for several front-ends of interest. In each case the SISO SNR (26) is 10 dB and the fading correlation matrix $\Sigma_{\mathbf{h}}$ is normalized by the attenuation in the SISO channel. Results are given for $M = N = 1 - 4$ antennas with spacings of $0.01\lambda \leq d \leq \lambda$, where λ is the carrier wavelength. The integrals in (4) and (5) are evaluated numerically and the results confirmed with Monte-Carlo simulations (not shown).

A. Antenna Array and Propagation Model

The receive array is a ULA of half-wavelength dipoles. Expressions for the impedance matrix and radiation pattern of such an array are available for infinitesimally thin wire dipoles [16], however, we prefer to evaluate finite-thickness

dipoles numerically. The Numerical Electromagnetics Code (NEC) [19], a well-known Method-of-Moments (MoM) based program, was used for this purpose. Each wire dipole is $10^{-3} \lambda$ thick and divided into 25 computational segments.

A sufficient condition for Rayleigh fading is that the received electric field be composed of a large number (in the sense of the central limit theorem) of plane waves modulated by independent and uniformly-distributed phases. We consider a two-dimensional model in which the plane waves are co-polarized with the dipole orientation and arrive with equal probability over the azimuthal range. The entries of the open-circuit correlation matrix $\Sigma_{\mathbf{h}}$ are then given by [20]

$$[\Sigma_{\mathbf{h}}]_{nm} = \frac{1}{2\pi} \int_0^{2\pi} g_n(\phi) g_m^*(\phi) e^{j2\pi \frac{d}{\lambda} (m-n) \cos \phi} d\phi, \quad (19)$$

where $g_n(\phi)$ is the voltage induced in the n^{th} antenna by a plane wave arriving with azimuthal angle ϕ .

The $g_n(\phi)$ functions were evaluated in NEC over 32 evenly spaced angles (for each inter-element spacing) and the results used in a numerical approximation of (19). This approach accounts for scattering between neighboring antennas – if we assumed the omnidirectionality of isolated dipoles, (19) would reduce to Clarke's [20] formula $J_0(2\pi \frac{d}{\lambda} (m-n))$, where $J_0(x)$ is the zeroth-order Bessel function of the first kind.

B. Noise Figure Example

Referring to Fig. 1, consider two uncoupled front-ends (label them "A" and "B") with identical impedance matrices

$$\begin{bmatrix} \mathbf{Z}_{11} & \mathbf{Z}_{12} \\ \mathbf{Z}_{21} & \mathbf{Z}_{22} \end{bmatrix} = \begin{bmatrix} z_{11} \mathbf{I} & \mathbf{0} \\ z_{21} \mathbf{I} & z_{22} \mathbf{I} \end{bmatrix}, \quad (20)$$

where $z_{11} = z_{22} = 50 \Omega$ and $z_{21} = 500 \Omega$, and uncorrelated noise sources $\Sigma_{12} = \Sigma_{21} = \mathbf{0}$, $\Sigma_{ii} = 4kT_0 B r_i$, $i \in \{1, 2\}$. Let the noise resistances of each front-end be assigned as

$$\begin{aligned} \text{Front-end A : } r_1 &= 9r_A, r_2 = 0 \\ \text{Front-end B : } r_1 &= 0, r_2 = 9r_A |G|^2, \end{aligned} \quad (21)$$

where $G = z_{21}/(z_A + z_{11})$ and $z_A = r_A + jx_A$ is the impedance of an isolated antenna. Note that the branches of both of these front-ends have a 10 dB noise figure, hence for uncoupled antennas they should produce identical capacities.

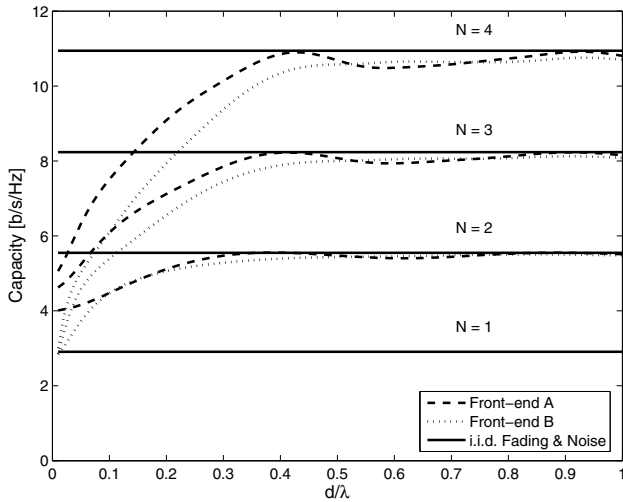


Fig. 3. Capacity versus inter-element spacing for two front-ends.

The capacity of each of these systems for $N = 1 - 4$ is shown in Fig. 3, with the i.i.d. fading and noise case (5) provided for reference. We immediately notice that for strongly coupled antennas (say, $d < 0.5\lambda$) these two front-ends behave quite differently, in stark contrast to the above statement for uncoupled antennas (which appears to be in agreement here for $d \geq 0.5\lambda$). In particular, a four-antenna receiver with $d = 0.1\lambda$ will benefit from a 25% increase in capacity by choosing front-end A over front-end B, even though they have the same noise figure. This somewhat peculiar result is understood by observing that the noise in front-end A correlates through the coupled antennas, while that of front-end B is isolated from the antennas and thus remains spatially white for all inter-element spacings. It is well-known that noise correlation can only increase capacity, thus front-end A should have a larger capacity at small spacings.

C. Matching Example

We now demonstrate an application of Theorem 2 for the receiver in Fig. 2. We selected a SiGe low-noise amplifier [21] designed for use in the cellular band. In high-gain mode with $R_{\text{bias}} = 510 \Omega$ and $f = 900$ MHz, its impedance matrix and Rothe-Dahlke noise parameters are:

$$\begin{bmatrix} z_{11} & z_{12} \\ z_{21} & z_{22} \end{bmatrix} = \begin{bmatrix} 35.7\angle -82.0^\circ & 2.74\angle 91.8^\circ \\ 325\angle 119^\circ & 46.1\angle -23.3^\circ \end{bmatrix} \Omega$$

$$r_a = 9.45 \Omega, \quad g_a = 3.24 \text{ mS}, \quad z_{\text{cor}} = 35.3\angle -114^\circ \Omega$$

An optimum matching network for this front-end is given in Theorem 2. While this network achieves the minimum noise factor matrix, it may be difficult to realize in practice. A practical, suboptimal alternative is to apply to each antenna the (two-port) optimal matching network (29) for an isolated dipole. We shall follow the terminology introduced in [10] and refer to this as *self-matching*.

Capacities for optimal and self-matching are shown in Fig. 4, with the i.i.d. fading and noise case again provided for

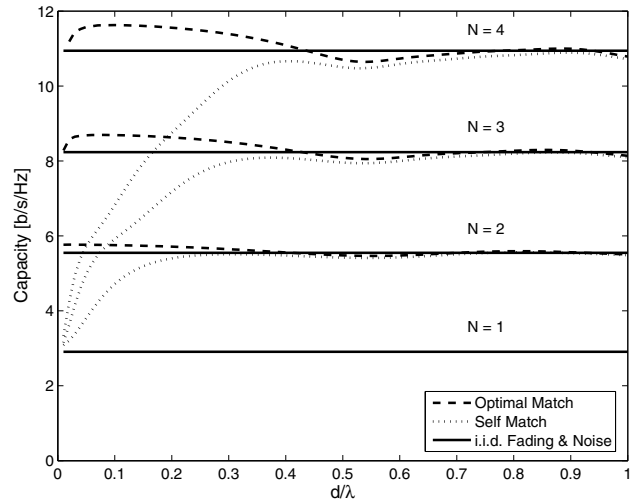


Fig. 4. Capacity for optimal and self matching.

reference. At small inter-element spacings, the optimal match is superior to the self match, and is an upper bound at all spacings in accordance with Theorem 2. For self-matching, the fading and noise correlations approach unity as the antennas are brought closer together, and the capacity reduces to that of a SISO system. In contrast, the optimal match is able to completely decouple the array at any distance, and the performance of an i.i.d. system is retained even at extremely close spacings.

The results for optimal matching should be interpreted with caution since the array may exhibit supergain behavior [12]. Consequently, the system is highly sensitive to channel estimation errors, and, as shown in² [22], becomes extremely narrowband at small inter-element spacings. In fact, this narrowband behavior may be used to explain the drop in the optimal match curve for $d < 0.1\lambda$ in Fig. 3 of [10] that is not observed here. The authors of [10] use a time-limited sinusoid in their finite-difference time-domain (FDTD) program, while here the MoM-based NEC assumes time-harmonic fields.

VII. CONCLUSION

We presented a circuit model for a linear, noisy MIMO receiver front-end and introduced the noise factor matrix \mathbf{F} as a natural extension of the noise factor of two-port networks. As a result we were able to derive theorems directly linking MIMO capacity to the eigenvalues of \mathbf{F} , which are analogous to the well-known concept of minimum noise figure design for SISO systems. Numerical examples were presented that demonstrated the inability of noise figure to predict performance in the presence of coupled antennas and the performance of the optimal multiport matching network for front-end amplifiers.

APPENDIX

A circuit model for a SISO receiver front-end is shown in Fig. 5. The antenna is modeled by a Thevenin equivalent

²In this study the match was optimized for power transfer instead of noise, however, the decoupling property responsible for these effects remains.

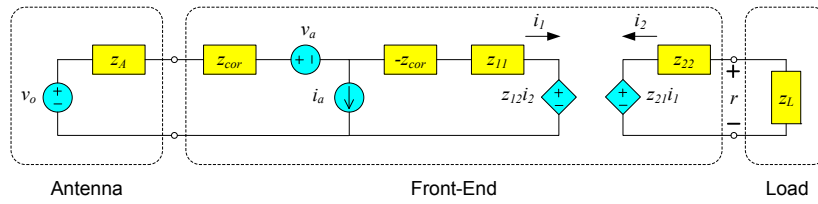


Fig. 5. Circuit model for a SISO receiver front-end.

circuit with impedance $z_A = r_A + jx_A$ and open-circuit voltage $v_o = h_o x + n_o$, where $h_o \sim \mathcal{CN}(0, 1)$ is (normalized) Rayleigh fading, x is the transmitted signal with $\mathbb{E}[|x|^2] = P$, and $n_o \sim \mathcal{CN}(0, 4kT_0Br_A)$ is antenna thermal noise.

The Rothe-Dahlke model [23], a commonly accepted standard for representing noisy, linear two-ports, is used to model the front-end. The noise sources $v_a \sim \mathcal{CN}(0, 4kT_0Br_a)$ and $i_a \sim \mathcal{CN}(0, 4kT_0Bg_a)$ are mutually independent, where r_a is the *equivalent noise resistance* and g_a is the *equivalent noise conductance*. Noise correlation between the input and output ports is accounted for by the *correlation impedance* z_{cor} .

The voltage across the load is

$$r = \frac{Gz_L}{z_{22} + z_L - Gz_{12}} (h_o x + n_o - z), \quad (22)$$

where $G = z_{21}/(z_A + z_{11})$ and $z = v_a + (z_A + z_{cor})i_a$. A useful metric associated with a two-port network is the *noise factor*,³ F , defined as the ratio of the output noise power to the (thermal) noise power contributed by the source alone. Identifying the noise component of r as $n \propto n_o - z$, we have

$$F = \frac{\mathbb{E}[|n|^2]}{\mathbb{E}[|n|^2]_{z=0}} = 1 + \frac{\mathbb{E}[|z|^2]}{4kT_0Br_A} \quad (23)$$

Now consider a lossless (and therefore noise-free) matching network with impedance matrix

$$\begin{bmatrix} z_{M11} & z_{M12} \\ z_{M21} & z_{M22} \end{bmatrix} \quad (24)$$

inserted between the antenna and front-end. The noise factor of the composite (matching plus front-end) network is

$$F = 1 + \frac{r_a + g_a |z'_A + z_{cor}|^2}{r'_A}, \quad (25)$$

where the transformed antenna impedance $z'_A = r'_A + jx'_A$ may be chosen arbitrarily with the appropriate matching network.

The SNR at the load is

$$\rho = \frac{P}{4kT_0Br_A F} = \frac{\rho_o}{F}, \quad (26)$$

where ρ_o is identified as the SNR at the open-circuited antenna terminal. Thus we can maximize ρ by minimizing (25). The minimum F_{\min} occurs at $z'_A = z_{\text{opt}} = r_{\text{opt}} + jx_{\text{opt}}$, where [23]

$$F_{\min} = 1 + 2 \left(g_a r_{cor} + \sqrt{g_a r_a + (g_a r_{cor})^2} \right) \quad (27)$$

$$z_{\text{opt}} = \sqrt{r_a/g_a + r_{cor}^2} - jx_{cor}. \quad (28)$$

³The *noise figure* of a two-port network is $10 \log_{10} F$.

One particular matching network that achieves $z'_A = z_{\text{opt}}$ is

$$\begin{bmatrix} z_{M11} & z_{M12} \\ z_{M21} & z_{M22} \end{bmatrix} = j \begin{bmatrix} -x_A & \sqrt{r_A r_{\text{opt}}} \\ \sqrt{r_A r_{\text{opt}}} & x_{\text{opt}} \end{bmatrix}. \quad (29)$$

REFERENCES

- [1] I. E. Telatar, "Capacity of multi-antenna Gaussian channels," *AT&T Bell Labs Internal Tech. Memo.*, Jun. 1995.
- [2] G. J. Foschini and M. J. Gans, "On limits of wireless communications in a fading environment when using multiple antennas," *Wireless Personal Commun.*, vol. 6, pp. 311-335, 1998.
- [3] M. Shafi *et al.*, ed., *IEEE J. Sel. Areas Commun.*, vol. 21, Apr. 2003.
- [4] —, *IEEE J. Sel. Areas Commun.*, vol. 21, Jun. 2003.
- [5] B. M. Hochwald *et al.*, ed., *IEEE Trans. Inform. Theory*, vol. 49, Oct. 2003.
- [6] D. Shiu *et al.*, "Fading correlation and its effect on the capacity of multielement antenna systems," *IEEE Trans. Commun.*, vol. 48, pp. 502-513, Mar. 2000.
- [7] X. Li and Z. Nie, "Mutual coupling effects on the performance of MIMO wireless channels," *IEEE Antennas Wireless Propag. Lett.*, vol. 3, pp. 344-347, 2004.
- [8] J. W. Wallace and M. A. Jensen, "Mutual coupling in MIMO wireless systems: A rigorous network theory analysis," *IEEE Trans. Wireless Commun.*, vol. 3, pp. 1317-1325, Jul. 2004.
- [9] A. Lozano, A. M. Tulino, and S. Verdu, "Multiple-antenna capacity in the low-power regime," *IEEE Trans. Inform. Theory*, vol. 49, pp. 2527-2544, Oct. 2003.
- [10] M. L. Morris and M. A. Jensen, "Network model for MIMO systems with coupled antennas and noisy amplifiers," *IEEE Trans. Antennas Propag.*, vol. 53 pp. 545-552, Jan. 2005.
- [11] M. J. Gans, "Channel capacity between antenna arrays – Part I: Sky noise dominates," *IEEE Trans. Commun.*, vol. 54, pp. 1586-1592, Sep. 2006.
- [12] —, "Channel capacity between antenna arrays – Part II: Amplifier noise dominates," *IEEE Trans. Commun.*, vol. 54, pp. 1983-1992, Nov. 2006.
- [13] R. A. Horn and C. R. Johnson, *Matrix Analysis*. New York: Cambridge, 1985.
- [14] M. Chiani, M. Z. Win, and A. Zanella, "On the capacity of spatially correlated MIMO Rayleigh-fading channels," *IEEE Trans. Inform. Theory*, vol. 49, no. 10, pp. 2363-2371, Oct. 2003.
- [15] H. A. Haus and R. B. Adler, *Circuit Theory of Linear Noisy Networks*. New York: Wiley, 1959.
- [16] C. A. Balanis, *Antenna Theory: Analysis and Design*, 3rd ed. New York: Wiley, 2005.
- [17] W. R. Bennett, *Electrical Noise*. New York: McGraw Hill, 1960.
- [18] R. Q. Twiss, "Nyquist's and Thevenin's theorems generalized for nonreciprocal linear networks," *J. Applied Physics*, vol. 26, pp. 599-602, May 1955.
- [19] G. J. Burke and A. J. Poggio, "Numerical Electromagnetics Code (NEC) – Method of moments," Tech. Doc. 11, Naval Ocean Systems Center, San Diego, CA, Jan. 1981.
- [20] R. H. Clarke, "A statistical theory of mobile-radio reception," *Bell Syst. Tech. J.*, vol. 47, pp. 957-1000, Jul. 1968.
- [21] <http://datasheets.maxim-ic.com/en/ds/MAX2642-MAX2643.pdf>
- [22] B. K. Lau *et al.*, "Impact of matching network on bandwidth of compact antenna arrays," *IEEE Trans. Antennas Propag.*, vol. 54, no. 11, pp. 3225-3238, Nov. 2006.
- [23] H. Rothe and W. Dahlke, "Theory of noisy fourpoles," *Proc. IRE*, vol. 44, pp. 811-818, Jun. 1956.